Modeling the Optimal Trajectory of a Skimmer Ship to Clean Oil Spills in the Open Sea

ARTICLE *in* SOCIETY OF PETROLEUM ENGINEERS JOURNAL · AUGUST 2015

DOI: 10.2118/174150-MS

3 AUTHORS, INCLUDING:

Susana Gómez

Universidad Nacional Autónoma de México

91 PUBLICATIONS **823** CITATIONS

SEE PROFILE

Benjamin Ivorra

Complutense University of Madrid

66 PUBLICATIONS **321** CITATIONS

SEE PROFILE

SPE-174150-MS

Modeling the Optimal Trajectory of a Skimmer Ship to clean Oil Spills in the Open Sea

Susana Gomez, Instituto de Matematicas Aplicadas y Sistemas, Universidad Nacional A. de Mexico, **Benjamin Ivorra**, Departamento de Matemática Aplicada & Instituto de Matemática Interdisciplinar, Universidad Complutense de Madrid, **Roland Glowinski**, Department of Mathematics, University of Houston, **Angel M. Ramos**, Departamento de Matemática Aplicada & Instituto de Matemática Interdisciplinar, Universidad Complutense de Madrid

This paper was prepared for presentation at the SPE Latin American and Caribbean Health, Safety, Environment and Sustainability Conference held in Bogot, Colombia, 78 July 2015

Abstract

Oil spill contamination in the open sea has been at the origin of some of the worst environmental disasters. One of the major cleaning techniques is the use of skimmer ships that contain various pumps distributed along its waterline to suck the oil from the surface of the water directly into storage units. We want to improve this process. We developed a model to simulate the effect of the skimmer ship on the evolution of the oil spill. This model, based on a finite volume approximation of an advection-diffusion-reaction equation, considers: the motion of oil spots resulting from the movement of the source of contamination; the diffusion and transport by wind and sea currents; and the phenomena associated with the action of the skimmer ship, assuming that it follows a pre-assigned trajectory. We introduce a nonlinear diffusion term to obtain finite speed diffusion. Also, we use an absorbing boundary condition, to account for the oil exiting the computational domain. To reduce numerical artificial diffusion, we use second order numerical schemes to discretize the advection terms. We also apply splitting schemes to decrease the computational complexity. To improve the whole process, we optimize the trajectory of a skimmer ship to maximize the amount of recovered oil during a fixed period of time, using an optimization method. The novel approach we advocate here is validated by comparing our numerical results with real life measurements from the Prestige spill, which took place in Spain in 2002. We were able to reproduce the satellite image of the spot after 4 days of pollution. We also prove that the optimal trajectory we get cleans the area near the coast up to 55 percent before the Prestige ship broke up. This percentage was improved to 88 percent by using a second ship on the entire area.

Keywords: Oil spill; Skimmer ship; Modelling; Advection-Reaction-Diffusion equation; Optimal trajectory.

1 Introduction

Oil spill contamination in the open sea has produced some of the worst environmental disasters in history [21]. In the case of the Prestige accident (Galicia, Spain 2002), more than 10 million gallons of crude oil were spilled [25] and polluted thousands of kilometers of coastline in Spain, France and Portugal [4]. This spill is considered the largest environmental disaster in the history of both Spain and Portugal and the cost of the disaster was evaluated to more than 770 million euros[18]. Because of its large geographical spread, the spill reached virtually all types of marine habitat, from offshore depths to shallow creeks. The worst affected habitats were in coastal areas, and this includes land damage caused by clean-up operations. Furthermore, this has economic repercussions on the inshore fishing and shellfish sector. The Prestige disaster was similar to that of the Exxon Valdez spill in terms of bird mortality, and it has been considered as one of the non-natural events most deadly to wildlife ever to have occurred in Europe. It was estimated that more than 50% of the sea birds and otters of the area were killed.

One of the major cleaning techniques [19,27] for these hazards is the use of skimmer ships [5]. Those ships use various pumps distributed along their waterline to suck the oil from the surface of the water directly into storage units. Those vessels move inside the oil spots to clean them as quickly as possible.

In order to be able to improve the efficiency of this pumping process, it is necessary first to simulate the movement of the spills both in space and time through a mathematical model. This movement is due to the effect of the displacement of the source of contamination, the diffusion caused by the difference in the density of the sea water and the oil and to the transport effect of the wind and sea currents. The pumping process of the skimmer ship, will also affect the transport of the pollutant. Also, an absorbing boundary condition has to be used to handle the possibility of the oil exiting the domain of study. We then proceed to model a trajectory for a skimmer ship, and using a global optimization evolutionary algorithm, we find the optimal trajectory to maximize the amount of oil pumped (i.e., minimizing the concentration of the remaining pollutant) on a fixed period of time. Here, two scenarios will be considered, the cleaning of the whole area under study, or giving priority to extract the oil near the coast.

The content of this article is as follows: In Section 2, we present the mathematical model we use to simulate the motion of the oil spots and the action of the skimmer ship and briefly introduce the numerical methods to be used for these simulations. In Section 3, we present the formulations of the objective functions to optimize the trajectory of the skimmer ship. In Section 4, the optimization method is described. In Section 5, we describe numerical experiments based on the 2002 Prestige oil spill data and discuss these results. Finally, some conclusions are made in Section 6

2 Mathematical model

We present here the mathematical model used to simulate the evolution of the oil spots concentration, due to the effects of the sea current, wind velocity fields and the pumping process during a time interval $(0,T)$, as previously introduced in [13].

We consider a spatial domain of simulation (also called computational domain) $\Omega \subset (x_{1,\min},x_{1,\max}) \times (x_{2,\min},x_{2,\max}) \subset \mathbb{R}^2$. The land domains are not included in Ω. We denote by $\partial\Omega_o$ the boundary of Ω in the open sea and by $\partial\Omega_c$ the boundary in the coast. We assume for simplicity that the density of the pollutant is smaller than the one of the sea water (so that it remains at the surface) and the layer-thickness of the pollutant is a known constant h. In practice, the value of h depends on the color of the oil in the water [22].

We denote by $c(x,t)$ the pollutant superficial concentration, measured as the amount of pollutant per surface area at $\{x,t\} \in \Omega \times (0,T)$. We assume that the evolution of c is governed by a source of contaminant which is taken as a circle of radius R_s that follows a trajectory $\zeta \in C^1([0,T],\mathbb{R}^2)$ and spills an amount of oil $S(t)$ per unit of time, by the effect of the diffusion of the pollutant, by the transport due to the wind and sea currents and also by the transport and sink due to the pumping process. Moreover, we assume that the skimmer ship follows a trajectory $\gamma \in C^1([0,T],\Omega)$.

From a practical point of view, a skimmer ship can be composed of multiple pumps, cleaning the water along the vessel waterline. For simplicity, we neglect the length of the ship compared to the size of Ω. We suppose also that there is only one pump, which is a circle of radius R_p, pumping the fluid with velocity Q in the radial direction.

In order to avoid the undesired effect of diffusion propagating at infinite speed, we control the velocity of the diffusion propagation using a nonlinear diffusion term. We have also included a boundary condition with appropriate absorbing properties to simulate the behavior of the computed solution near the boundary of the computational domain.

This model is given by

$$
\begin{cases}
\dfrac{\partial c}{\partial t} - \nabla\cdot\dfrac{c^\kappa}{c_{\text{ref}}^\kappa}\mathbf{d}\nabla c + \nabla\cdot c\,\mathbf{w} + \nabla\cdot c\,\mathbf{s} \\
\qquad\qquad +\nabla\cdot c\,\mathbf{p}_{\text{tol}} = -\dfrac{2Q}{R_p}\,c\;\chi_{B(\gamma(t),R_p)} \\
\qquad\qquad\qquad +\dfrac{S}{2\pi R_S}\chi_{B(\zeta(t),R_s)}, & \text{in } \Omega\times(0,T), \\
L\dfrac{\partial c}{\partial t} + \Big[-(\mathbf{w}+\mathbf{s}+\mathbf{p}_{\text{tol}})c + \dfrac{c^\kappa}{c_{\text{ref}}^\kappa}\mathbf{d}\nabla c\Big]\cdot\mathbf{n} = 0, & \text{on } \partial\Omega_o\times(0,T), \\
\Big(\dfrac{c^\kappa}{c_{\text{ref}}^\kappa}\mathbf{d}\nabla c\Big)\cdot\mathbf{n} = 0, & \text{on } \partial\Omega_c\times(0,T), \\
c(0) = c_0,
\end{cases}
\tag{1}
$$

where:

- $B(a,b)$ is the ball of center a and radius b.
- $\chi_{B(a,b)}(x) = \begin{cases} 0, & \text{if } x \in \Omega\backslash B(a,b), \\ 1, & \text{if } x \in B(a,b). \end{cases}$
- The function c_0 is the initial superficial concentration; we assume that c_0 has a compact support in Ω.
- $\mathbf{d} = \begin{pmatrix} d_1 & 0 \\ 0 & d_2 \end{pmatrix}$, d_1, d_2 (both >0) being the diffusion coefficients in the west-east and south-north directions.
- $\mathbf{w}$ is the horizontal components of the wind velocity multiplied by a suitable drag factor.
- $\mathbf{s}$ is the see current velocity.
- $\mathbf{p}_{\text{tol}}(\xi,t) = \max\Big(\dfrac{\|\mathbf{p}(\xi,t)\|_2 - \text{tol}}{Q-\text{tol}}, 0\Big)\cdot\mathbf{p}(\xi,t)$ is a corrected approximation of the velocity pump $\mathbf{p}(\xi,t) = QR_p\dfrac{\overrightarrow{\gamma(t)\xi}}{(\|\overrightarrow{\gamma(t)\xi}\|_2)^2}$, if $\xi \in \Omega\backslash B(\gamma(t),R_p)$, and 0, elsewhere [2]. This expression means that (i) the effect of the velocity field $\mathbf{p}$ on oil particles is neglected

(i.e., $\mathbf{p}_{\text{tol}} = 0$) when $\|\mathbf{p}(\xi,t)\|_2 <$tol, for which the pump velocity is considered negligible regarding the diffusion coefficients; (ii) $\mathbf{p}_{\text{tol}}(\xi,t) = \mathbf{p}(\xi,t)$, when $\|\overrightarrow{\gamma(t)\xi}\|_2 \leq R_p$; and (iii) $\mathbf{p}_{\text{tol}}(\xi,t) < \mathbf{p}(\xi,t)$ and $\mathbf{p}_{\text{tol}}(\xi,t)$ is a smooth function, when $\|\overrightarrow{\gamma(t)\xi}\|_2 > R_p$.

- c_{ref} is a reference pollutant concentration (here, $c_{\text{ref}} = 1$), and $\kappa > 0$ (typical values of κ being 1, 2 and 3).
- $L = \sqrt{(x_{\max} - x_{\min})^2 + (y_{\max} - y_{\min})^2}$ is the characteristic size of the domain Ω.

For the numerical solution of this equation, we use a finite volume discretization method and to reduce the computational time required by our simulations, we use an operator-splitting approach for the pumping term $\nabla \cdot c\,\mathbf{p}_{\text{tol}}$. Furthermore, to limit the artificial diffusion effect typical of this kind of numerical model [9], we use second order accurate time discretization schemes with nonlinear limiters to treat the advection. The full scheme of the considered numerical model can be found in [13].

3 Optimal trajectory

As mentioned in Section 1, we address the problem of finding an optimal trajectory for the skimmer ship, for a particular oil contamination scenario during a fixed time interval $(0,T)$.

From a general point of view, we consider optimization problems of the form:

$$\min_{\gamma \in D_c} J_c(\gamma) \tag{2}$$

where $J_c(\gamma)$ is the original version of the objective function that will be defined below according to the considered problem, $D_c = \{\gamma \in C^1([0,T],\Omega)$ such that $|\gamma'(t)| \leq V_{\max}, \forall t \in [0,T]\}$ is the feasible region and $V_{\max}$ is the maximum speed of the ship when performing the pumping process. This restriction on the speed of γ avoids to consider trajectories implying non realistic ship velocities.

During this work we have considered two particular optimization problems associated to two different formulations of the objective function $J_c(.)$

- For the given time T, we minimize the concentration $c(\xi,T)$ of the remaining pollutant in Ω, which is equivalent to maximize the amount of pumped oil from the sea. In this case

$$J_c(\gamma) = \int_0^T \Big(S(\tau) - c(\tau,\gamma(\tau))2\pi R_p Q\Big)\mathrm{d}\tau. \tag{3}$$

- For the given time T, we want to prioritize minimizing the pollutant concentration near the coast. To do so, we consider

$$J_c(\gamma) = \int_0^T \int_\Omega \text{coef}(x)c(\tau,x)\mathrm{d}x\mathrm{d}\tau, \tag{4}$$

where $\text{coef}(x) = \lambda_1\Big(1 - \big(\text{dist}(x)/\max_{x\in\Omega}\text{dist}(x)\big)\Big)^{\lambda_2} + \lambda_3$ is a weight function, with $\text{dist}(x)$ being the distance (in meters) between x and the nearest point in $\partial\Omega_c$, λ_1, λ_2 and λ_3 are real parameters used to control the behavior of coef(.). Function coef(.) is used to generate coefficients that give more weight to the value of c for the points near the coast than for the points far from the coast.

These formulations take into consideration the evolution in time and space of the pollution concentration (obtained by solving the model), and specifically in the case of formulation (4) where the distances between the oil spots and the coast are then variable.

In order to find numerically a smooth optimal pump trajectory (i.e., without sharp corners), we consider trajectories built by using cubic spline interpolation through $n_{\text{npi}} \in \mathbb{N}$ 2-D interpolation points.

The set of interpolation points, denoted by P_{int}, is constructed by using a polar representation:

$$P_{\text{int}} = \{(r_1,\theta_1),...,(r_{n_{\text{npi}}},\theta_{n_{\text{npi}}})\},$$

where $r_i \in [0, r_{\max}]$, with $r_{\max} = V_{\max} * (T/n_{\text{npi}})$ (modeling the ship velocity constraint), and $\theta_i \in [0,2\pi)$, for $i = 1,...,n_{\text{npi}}$.

Given an interpolation point expressed in Cartesian coordinates $(x_k^{\text{int}}, y_k^{\text{int}})$, with $k \in \{1,...,n_{\text{npi}}-1\}$, the next one $(x_{k+1}^{\text{int}}, y_{k+1}^{\text{int}})$ is built as:

$$\begin{aligned} x_{k+1}^{\text{int}} &= x_k^{\text{int}} + r_k\cos(\theta_k), \\ y_{k+1}^{\text{int}} &= y_k^{\text{int}} + r_k\sin(\theta_k). \end{aligned}$$

The resulting interpolated trajectory is denoted by $\gamma_{(r_i,\theta_i)}$.

Furthermore, we need to avoid the ship leaving the domain of study Ω. To accomplish this, we project the trajectory $\gamma_{(r_i,\theta_i)}$ using an orthogonal projector on Ω, called Pr_Ω, defined as:

$$\begin{aligned} \text{Pr}_\Omega(\gamma_{(r_i,\theta_i)}(\tau)) = \Big(&\max(\min(\gamma_x(\tau),x_{\max}),x_{\min}), \\ &\max(\min(\gamma_y(\tau),y_{\max}),y_{\min})\Big). \end{aligned} \tag{5}$$

Thus, the numerical optimization problem that we solve, is of the form:

$$\begin{aligned} &\min J(r_i,\theta_i)\\ &\text{subject to}\\ &\quad 0\le r_i\le r_{\max} \quad ,i=1,...,n_{\text{npi}},\\ &\quad 0\le \theta_i<2\pi \quad ,i=1,...,n_{\text{npi}}, \end{aligned} \tag{6}$$

where $J(\{r_i,\theta_i\}_{i=1}^{\text{npi}})$ is the considered version of the objective function $J_c(\gamma)$ and $\{(r_i,\theta_i)\}_{i=1}^{n_{\text{npi}}}\subset D$ are the optimization variables (in this case, unknown coordinates of the trajectory of the skimmer ship) where $D=[0,r_{\max}]\times[0,2\pi)$ is the feasible region. The total number of optimization variables is $N=2n_{\text{npi}}$. Furthermore, if J_c is defined by formulation (3) then

$$J(\{r_i,\theta_i\}_{i=1}^{\text{npi}})=\int_0^T\Big(S(\tau)-c(\tau,\gamma_{(r_i,\theta_i)}(\tau))2\pi R_pQ\Big)\mathrm{d}\tau,$$

and if J_c is defined by formulation (4) then

$$J(\{r_i,\theta_i\}_{i=1}^{\text{npi}})=\int_0^T\int_\Omega \text{coef}(x)c(\tau,x)\mathrm{d}x\mathrm{d}\tau.$$

Since problem (6) has many local and global minima [11], we need to use a global optimization method capable to find one global solution.

4 Global optimization method

In order to solve optimization Problem (6), we develop an hybrid global optimization method. This method is based on the combination of a particular Genetic Algorithm (GA) [10,12,26] and a Multi-layer line search algorithm [15,17] to improve the GA performance. In addition, to reduce the computational time required by the optimization process, we have designed a parallel version of this method.

4.1 Genetic Algorithm Genetic algorithms (GA) are a class of Evolutionary meta-heuristic Optimization Algorithms which apply the principles of natural evolution to find an optimal solution of an optimization problem. In particular, for numerical optimization problems on continuous domains of $\mathbb{R}^N$, where $N\in\mathbb{N}$ is the number of optimization variables, real-coded GAs (i.e., GAs working with points, in the feasible region, represented by real vectors) are well suited.

In a GA, a first set of $N_{\text{p}}=50$ points (called 'Individuals') is randomly generated inside the feasible region $D\subset\mathbb{R}^N$. This set is called the 'Initial Population' and denoted by $X^0=\{x_l^0\in D,l=1,...,N_{\text{p}}\}$. Throughout this section, all random numbers are generated by considering a uniform distribution in (0, 1) .

Then, the objective function is evaluated for each individual of the population. Next, to improve recursively N_{g} times the population, three stochastic operators are used: selection, crossover and mutation. Each time a new population is created, it is called a 'Generation'. A thorough calibration of the parameters and operators of the algorithm, has been reported in [11] for this application. Here, we give a brief description of the final algorithm. While the number of generations is less than the maximum allowed $N_g=50$, for each population we perform the following operators:

- Selection to determine which individuals are selected to participate in the Crossover process. For our problem, we use the binary tournament without replacement selection operator, which is suitable for handling the existence of a large number of local minima. With this choice, the best individual is selected twice and the worst one is eliminated. This guarantees that the individuals with better objective function value have higher probability to be selected. However, this operator also has diversity in order to avoid a premature convergence of the algorithm to a local minimum.

- Crossover to recombine pairs of individuals selected in the previous step to generate new individuals. In our case, we want to achieve diversity, and therefore we use a parent-centric crossover called best combinatorial crossover.

- Mutation of the resulting population, to increase diversity while checking that the new individual remains in the feasible domain. Here we use a non-uniform mutation which allows to explore the feasible domain uniformly in the first generations, and locally in later generations.

- The best individual (i.e., with the lowest objective function value) found until this step is directly copied in the new generation.

- Evaluation of the objective function for each new individual of the population.

An optimal solution to the considered problem is given by the individual with the lowest objective function value after the last generation.

4.2 Hybrid GA Secant Method It is well known (see [24]) that the initial population may strongly affect the efficiency of GAs and that a "good" initial population should combine genetic diversity (i.e., the ability to reach the whole feasible space during the evolution process) with uniform coverage (i.e., a spatial distribution in the feasible space which avoids clustering and uncovered regions).

Taking this into account, we present an hybrid optimization method based on the successive execution of the GA, starting from initial populations which are recursively improved. More precisely, at the beginning the GA is run N_g generations starting from a totally random initial population denoted by $X_1^0 = \{x_{1,j}^0 \in D, j = 1,...,N_p\}$. At the end of this run, we denote $o_1 \in D$ the best individual obtained by the GA. Then, we perform secant line searches starting from each individual x_j^0, with $j = 1,...,N_p$, along the direction $\overrightarrow{x_j^1 o_1}$. Those line searches generate a set of $N_p - 1$ new individuals, denoted $X_2^S = \{x_{2,j}^0 \in D, j = 1,...,N_{p-1}\}$. Then, we consider $X_2^0 = X_2^S \cup \{o_1\}$ that is used as the initial population for another run of the GA, and this process will be repeated recursively $N_{Sec} = 6$ number of times.

This algorithm, called Hybrid GA Multi-layer line search Algorithm (HGMA), has been reported and validated on various industrial problems in [11,14,15,16,17].

4.3 Parallelization of the HGMA In the above mentioned algorithm, each time a generation is performed, it is necessary to evaluate the objective function value for each individual in the population, and this implies to compute the solution of model (2). This is a very time consuming process, and it is then necessary to parallelize the HGMA to improve the computational speed. This parallelization is performed by using a new operator called migration.

The parallel process consists in dividing the population among a number of processors $N_{proc} = 16$. A HGMA will be performed on each processor. Then, a migration process will send the best individuals of processor P_i to processor P_{i+1} replacing the same number of individuals. Three different migration schemes were tested over a set of synthetic examples presented in [2], that mimic real situations: 1) the case of two spots of small size, 2) a set of three finger shaped spots and 3) the case of a large spot. The migration scheme that showed better performance consists in processor P_i sending the best $N_i = 10$ individuals to processor P_{i+1} replacing the worst individuals. The results of the parallelization using 16 processors, showed that for case 1 the run to find the optimal trajectory, took in sequential mode 3 hours and 15 minutes, whereas in parallel mode the run lasted 9 minutes. For case 2, the sequential process took 18 hours and 31 minutes and it run in 18 minutes in parallel. In case 3, it took 3 hours and 31 minutes for one processor and 15 minutes for 16 processors.

We will use this parallel migration process to generate the results that will be presented in the next section.

5 Numerical experiments

In this Section, we present the numerical experiments used to check the ability of the model to reproduce real observations and the efficiency of the optimization approach presented previously. The first experiment, presented in Section 5.1, aims to validate the oil concentration evolution predicted by our model when no pumping process is considered. To do so, we compare the model result with a real satellite image of the Prestige spill hazard. Then in Section 5.2, we solve several optimization problems of the form (2) with the methodology presented in Section 5.2 and analyze the behavior of the solution regarding some key parameters.

5.1 Model validation Before solving optimal trajectory problems in the next Section 5.2, we first want to study the validity of the evolution of the oil concentration predicted by our model applied to the Prestige hazard.

We consider model (1) without the pumping process (i.e., we set $Q = 0$). Then, we simulate the oil concentration evolution from the beginning of the Prestige event on the 13th to the 17th of November 2002 (at this day the only available clear satellite image of the situation was taken, before the Prestige ship broke up). Considering this time interval, we use the following model parameters:

- $\Omega \subset [-12.5, -7.5] \times [42, 44.5]$ (in longitude-latitude coordinate system) which is assumed to be large enough to avoid the oil concentration leaving this domain during the considered time interval. Ω and the considered Spanish land are presented on Figure 1.
- The velocity fields $\mathbf{w}$ and $\mathbf{s}$ are estimated by considering historical discrete data provided by the research center Mercator Ocean (Website: `http://www.mercator-ocean.fr`) and completed by 3D spline interpolation to be able to obtain values at points with no data.
- The diffusion coefficient d is set to $0.5(\text{m.s}^{-1})$ [2,7].
- The trajectory followed by the Prestige ship was taken from the literature [6,20].
- To our knowledge, the exact amount of oil S spilled by the Prestige ship into the ocean remains unknown [1,6,20]. It is only known that around 54.000 tons of oil were spilled into the sea before the Prestige ship broke on the 19th of November 2002. We have then used the value of $S(t) = 22(kg.s^{-1}), \forall t$, (by taking $R_s = 1$ (m)).
- $\kappa = 1$ [13].
- For the numerical finite volume scheme used to approximate the solution of model (1), we consider a 100×100 spatial mesh and a time step of 1 hour. All other parameters are given in [13].

Taking into consideration those values, we present in Figure 1 the solution given by our numerical model on the 17th of November 2002. In the same figure, we also show the satellite image taken by the Envisat ASAR satellite (property of the European Spatial Agency, Website: `https://earth.esa.int/web/guest/-/prestige-oil-spill-galicia-spain-1623`) at the same date. We can observe that graphically both images present similarities regarding the general behavior of the oil spill shape. This indicates that our model predicts well the evolution of the oil concentration of the Prestige case. However, this figure also illustrates the limitations of our model which omits to consider some complex physical effects of the sea currents on the oil spill. For instance, our model fails to predict the splitting of the main oil spot in two branches.

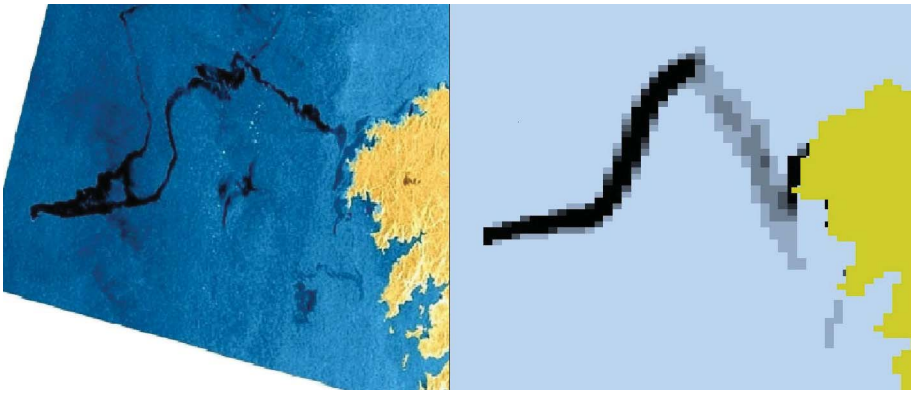

Figure 1: (Left) Satellite image of the Prestige oil spill situation taken by the Envisat ASAR satellite (European Spatial Agency) at 17 November 2002. (Right) Oil concentration simulated by the model presented in this work for the same date. The coast is also represented in green.

5.2 Trajectory Optimization We are now interested in applying the optimization method presented in this paper to solve several optimal trajectory problems of the skimmer ship by considering the Prestige hazard framework. Those problems are designed to study the impact of the optimal trajectories considering the objective function formulations (3) or (4) and several values of the pump power.

5.2.1 Considered problems We study the Prestige hazard with the model parameters presented in Section 5.1. However, the model is now run up from the 13th to the 19th of November 2002 (i.e., the date when the Prestige ship broke up). Furthermore, to reduce the computational time required by the optimization process, we use a 50×50 spatial mesh and a time step of 1 hour 30 minutes for the numerical finite volume scheme. The amount of the concentration of oil in the open sea (without pumping) simulated by the model and the trajectory followed by the Prestige ship are presented on Figure 2. Furthermore, on the same figure, we also give a 3D representation of the oil concentration in order to visualize the reduction of the maximum amount of oil contamination in Ω. For this reason and for now on, each time the oil concentration is shown the 3D representation is also displayed.

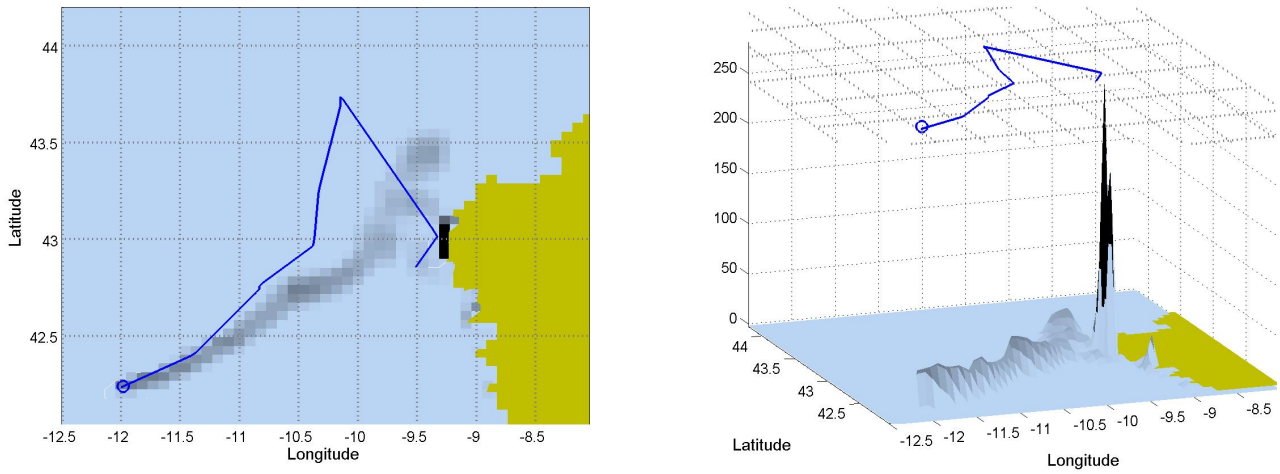

Figure 2: (Top) Top view and (Bottom) 3D view of the final oil concentration distribution at the 19th of November 2002. Furthermore the trajectory of the Prestige ship (continuous line) and the final position of the Prestige ship (o) are also presented.

Now, we activate the pumping process by considering three levels of pumping power Q=0.3 (m s^{-1}), 4 (m s^{-1}) and 8 (m s^{-1}). More precisely:

- This first value of $Q = 0.3$ corresponds to the 'Controlled Floating Skimmer' system build by the Novetec group (Website: `http://novetec.es/body_skimmer.htm`). This device has the advantage of allowing the skimmer ship to pump oil in movement.

- The highest value of $Q = 8$ is similar to the global pumping capacity used by the biggest skimmer ship available at this date: the A-whale. Website: `http://www.marketwatch.com/story/bp-tests-taiwanese-oil-skimming-ship-2010-07-04`.

  Although the global pumping system is one of the most powerful, due to technical restrictions this ship cannot perform pumping in movement. Furthermore, it has only be used once during the Gulf of Mexico Deepwater Horizon oil spill disaster in 2010 and was proven inefficient (see: `http://af.reuters.com/article/energyOilNews/idAFN1614683620100716`). However, here we consider such a powerful system by assuming that it performs the cleaning task in movement.

- Finally, the intermediate value of $Q = 4$ is considered in order to study the interest of an intermediate pumping power between the A-Whale and the Controlled Floating Skimmer system.

For each value of the pumping power Q, we solve the numerical trajectory Problem (6) using both formulations of the objective function (3) and (4). For the (4) case, we set λ_1 =20, $\lambda_2 = 4$ and $\lambda_3 = 1$ in order to impose strong weights to the oil spots near the coast, forcing the ship to remain there. A graphical representation of function coef(.) with those coefficients is given on Figure 3. The skimmer ship trajectory starts from the position (-9.4,42.75) (longitude, latitude) and is parametrized by 5 interpolation points (obtained using the optimization method) with $V_{\max}$=10 (km.h^{-1}) [11]. To simplify notation, those experiments are denoted by **OPT-Q-F**, where **Q** is replaced by the value of parameter Q and **F** by the type of objective function used.

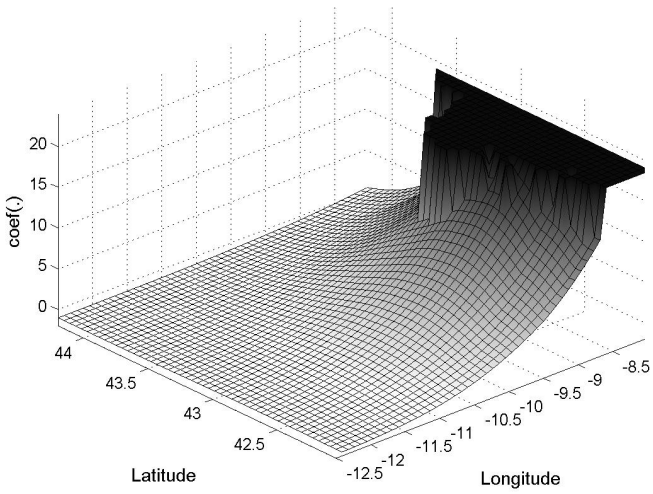

Figure 3: Graphical representation of the function coef(.) with λ_1 =20, $\lambda_2 = 4$ and $\lambda_3 = 1$.

In order to study the advantage of the optimized results obtained here, we compare the objective function values obtained with the computed optimal trajectories, with the straightforward trajectory that simply follows the Prestige ship (this trajectory seems to be the first intuitive option taken by the authorities in the case of oil spill accidents). We make this comparison using different values of the pumping power Q and starting the trajectory from position (-9.4,42.75), reaching the Prestige ship (at speed $V_{\max}$) and then following exactly the Prestige ship. These experiments are denoted by **PT-Q-**(3) and **PT-Q-**(4), according to the objective function formulation. Notation **PT** means following the Prestige Trajectory.

5.2.2 Results We first present and analyze the results obtained when considering the objective function formulation (3), that aims to reduce the amount of oil over the entire area. In that case, the considered experiments are **OPT-0.3-**(3), **OPT-4-**(3), **OPT-8-**(3), **PT-0.3-**(3), **PT-4-**(3) and **PT-8-**(3). We recall that without pumping the final amount of spilled oil on the 19th of November 2002 (i.e., the final value of the objective function considering **E-0-**(3)) is around 54000 tons of oil. The optimal trajectory found and the obtained final oil concentration distribution are presented in Figures 4 and 5. The final values of the objective function (3) (i.e., the amount (in

Exp.	**OPT-0.3-**(3)	**OPT-4-**(3)	**OPT-8-**(3)
O. Func.	50915	32241	31627
Reduc.	6	40	42
Exp.	**PT-0.3-**(3)	**PT-4-**(3)	**PT-8-**(3)
O. Func.	52712	36968	23574
Reduc.	2	31	56

Table 1: Objective function (3) **value (O. Func.) expressed in tons of oil and the percent of oil pumped (Reduc.) given by the experiments (Exp.): OPT-0.3-**(3)**, OPT-4-**(3)**, OPT-8-**(3)**, PT-0.3-**(3)**, PT-4-**(3) **and PT-8-**(3)

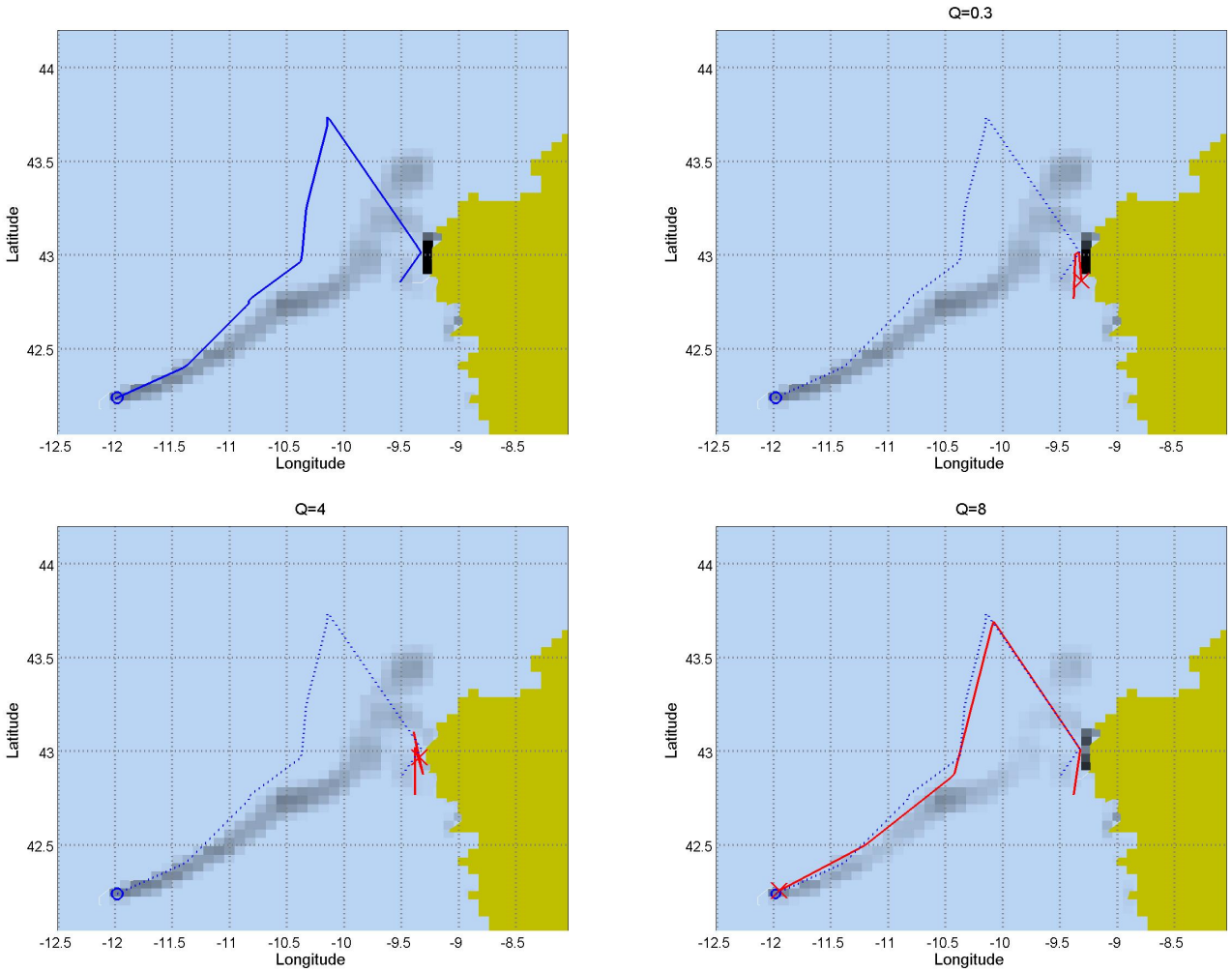

Figure 4: Top view of the final oil concentration distribution at 19 November 2002, skimmer ship trajectory (continuous red line), final position of the skimmer ship (x) and final position of the Prestige ship (o) for the experiments: (Top-Left) trajectory of the Prestige ship (continuous blue line) with no pumping process, (Top-Right) OPT-0.3-(3)**, (Bottom-Left) OPT-4-**(3) **and (Bottom Right) OPT-8-**(3)**. The trajectory of the Prestige ship is presented in dotted blue line.**

tons) of oil remaining in the sea at the final date) and the reduction in percentage of this value regarding the scenario without skimmer ship are given in Table 1.

As we can see on Table 1, for the scenarios of pumping power Q=0.3 and Q=4, the optimized trajectories give better results than following the Prestige ship (**OPT** vs **PT**). We can observe on Figure 4 and 5, that in both cases the skimmer ship remains close to the coast as, due to the sea and wind currents, a large amount of oil is reaching the coast. On the contrary, in the case of the most powerful pump (i.e., Q=8), the optimized trajectory is less efficient than following directly the Prestige ship. However, regarding the optimized trajectory for this case, we note a similar graphical behavior than the trajectory of the Prestige ship. This seems to indicate that the optimization process try to reproduce this particular trajectory. However, due to the reduced number of interpolation

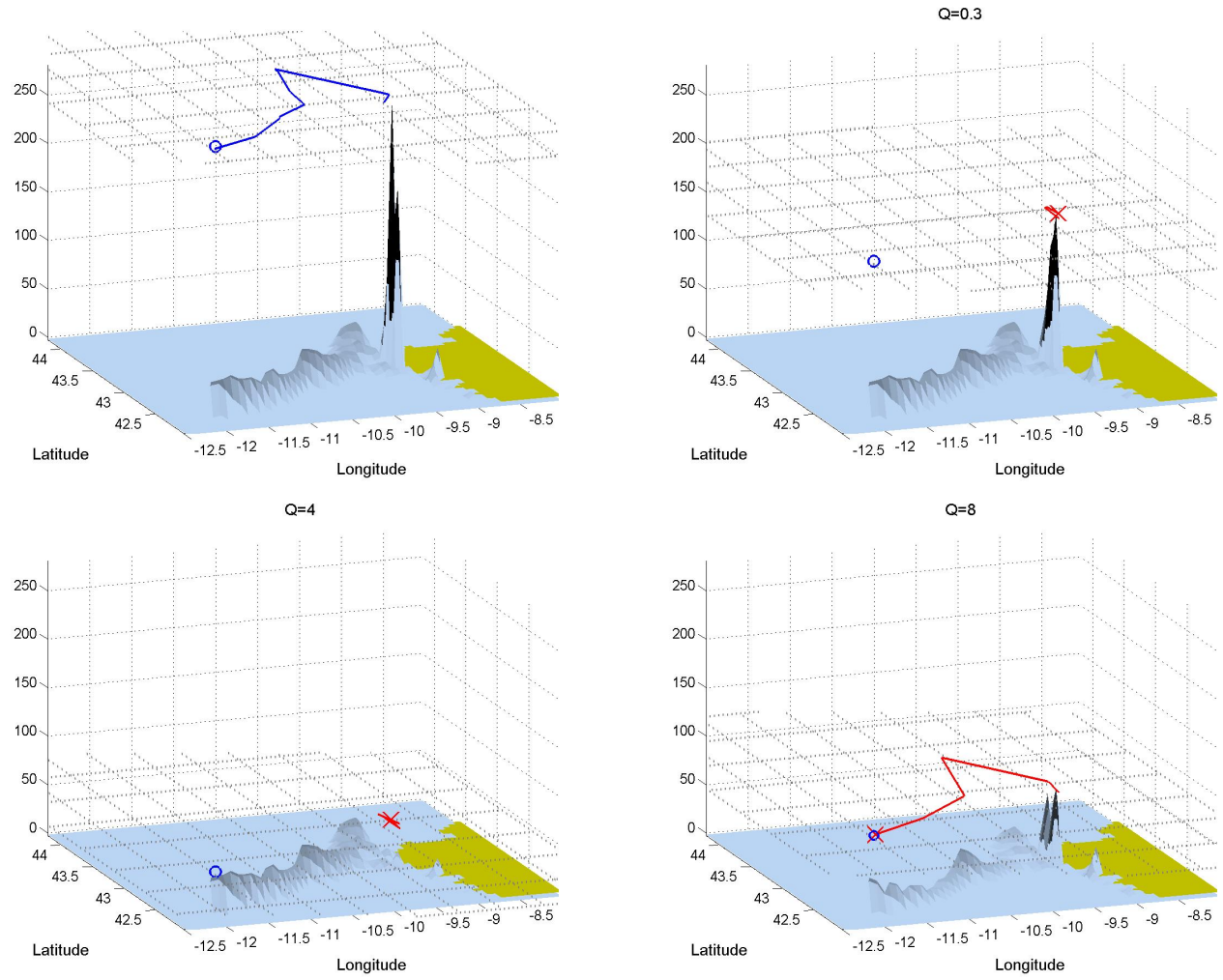

Figure 5: 3D view of the final oil concentration distribution on the 19th of November 2002 for the experiments: (Top-Left) case with no pumping process, (Top-Right) OPT-0.3-(3), (Bottom-Left) OPT-4-(3) and (Bottom Right) OPT-8-(3). A plane at the same height as the maximum value of the oil concentration is also presented. In this plane the skimmer ship trajectory (continuous red line), the Prestige ship trajectory when there is no pumping process (continuous blue line), final position of the skimmer ship (x) and final position of the Prestige ship (o) are depicted.

points (optimization variables), there exist some discrepancy between both trajectories, which explains the differences observed in the final results. All those results tend to show that up to a certain pump power, following the source of contamination is not the best option. An optimization process should be used in order to analyze which trajectory should be preferred. Another indication which can be derived from those experiments is that the efficiency of the cleaning process is not linearly proportional to the pump power. Indeed, with $Q = 4$ we found a result quasi as efficient as for Q=8. We can deduce that instead of using one powerful skimmer system, various systems of less power should be preferred. This conclusion is similar to what was observed during the Gulf of Mexico Deepwater Horizon oil spill disaster in 2010 where the A-Whale skimmer ship was used but was experimentally demonstrated less efficient (due to restrictions in its movements and difficulties to control its pumping process) than other skimmer ships of less power (see: `http://af.reuters.com/article/energyOilNews/idAFN1614683620100716`).

We now focus on the results obtained with the formulation (4) and the experiments **OPT-0.3-**(4), **OPT-4-**(4), **OPT-8-**(4), versus following the Prestige trajectory **PT-0.3-**(4), **PT-4-**(4) and **PT-8-**(4). In that case, the weighted final amount of rejected oil (or the final value of the objective function considering OPT-0-(4)) is around 2.413e+10. The optimal trajectories found at the end of these experiments and the final weighted oil concentration distribution, defined as $c_w(x) = \int_0^T \text{coef}(x)c(\tau,x)\text{d}\tau$, are presented on Figures 6 and 7. The final values of the objective function (4) and the reduction in percentage of this value with respect to the scenario without pumping are given in Table 2. In addition, we also present the final oil concentration distribution c on Figures 8 and 9. Finally, the final values of the objective function (3) and the reduction in percentage of this value with respect to the scenario without pumping are given in Table 3.

As we can observe on Figures 6 and 7, that in all cases the optimized trajectories remain near the coast, which was expected from the

Exp.	**OPT-0.3-**(4)	**OPT-4-**(4)	**OPT-8-**(4)
O. Func.	2.144e10	1.366e10	1.105e10
Reduc.	11	43	55
Exp.	**PT-0.3-**(4)	**PT-4-**(4)	**PT-8-**(4)
O. Func.	2.3632e10	2.2057e10	1.330e+10
Reduc.	2	9	45

Table 2: Objective function (4) **value (O. Func.) and percentage reduction (Reduc.) of this value regarding the scenario Q=0 given by the experiments (Exp.): OPT-0.3-**(4)**, OPT-4-**(4)**, OPT-8-**(4)**, PT-0.3-**(4)**, PT-4-**(4) **and PT-8-**(4)**.**

Exp.	**OPT-0.3-**(4)	**OPT-4-**(4)	**OPT-8-**(4)
O. Func.	50973	41233	40136
Reduc.	6	24	26
Exp.	**PT-0.3-**(4)	**PT-4-**(4)	**PT-8-**(4)
O. Func.	52712	36968	23574
Reduc.	2	31	56

Table 3: Objective function (3) **value (O. Func.) expressed in tons of oil and the percent reduction (Reduc.) of this value regarding the scenario Q=0 given by the experiments (Exp.): OPT-0.3-**(4)**, OPT-4-**(4)**, OPT-8-**(4)**, PT-0.3-**(4)**, PT-4-**(4) **and PT-8-**(4)**.**

definition of the cost function (4). Regarding the final values of the objective functions presented on Table 3, we see that all optimized trajectories give better results (i.e, lower objective function values) than the trajectory following the Prestige ship. Even in the scenario of using the most powerful pump Q=8, when following the Prestige ship the amount of oil escaping from the pumping process generates important contamination on the coast. This seems to indicate that in the cases when protecting the coast is the objective, the best strategy is to concentrate the cleaning effort around the coast. Regarding the amount of remaining oil in sea reported on Table 3, we see, as expected, that those values are worst than considering the optimization process with formulation (3).

Regarding the final oil concentration depicted in Figures 8 and 9, we observe that the contamination has been reduced near the coast but remains unchanged in the open sea. Thus, a better option should be to clean both coast and open sea. For instance, we can use a skimmer ship following the Prestige boat and other skimmer ship following the optimal trajectory using objective function (4). In order to illustrate this idea, we consider two skimmer ships with Q =8 (m.s^{-1}), one following the trajectory given by **OPT-8-**(4) and other one following the Prestige ship. In that case, the final amount of oil remaining in the sea is 11837 tons, which represents a decrease of 88% of this value without pumping. The final oil concentration distribution c is presented on Figure 10, where we can observe the drastic global reduction of oil contamination in the whole domain. This result shows that this last strategy is effective to clean the oil spill.

6 Conclusions

In this article we have used an improved version of the mathematical model discussed in [2,11,13], for simulating the movement of oil spills in the open sea, taking into account wind, sea currents, the motion of the contamination source, the effect of a skimmer ship used for the oil cleaning by pumping. This model has been designed to control the artificial diffusivity, the velocity of the diffusion propagation, and the behavior of the computed solution at the boundary of the computational domain.

With this model, without considering the pumping process, we were able to reproduce the movement of the spill produced by the Prestige vessel in 2002 in Spain, on the first 4 days.

To obtain optimal trajectories for a skimmer ship pumping the oil, we have designed two different objective functions: one where the optimal trajectory is searched over the whole area of study, and a second formulation of the objective function that is designed to clean the coast. This second formulation uses a weighted objective function, to give more importance to the pollution near the coast. We then use a suitable hybrid evolutionary optimization algorithm, to find the optimal trajectories for these two different formulations. We have compared the obtained optimal trajectories with the trajectory that follows the Prestige vessel, using three different pumping power alternatives. The results show that when the general formulation of the objective function does not artificially force to remain near the coast, the optimal trajectories remain near the coast anyway (as the highest concentration of oil has gone there because of the effect of the wind and sea currents), for small or medium pumping power, whereas for high pumping power, the optimal trajectory seems to follow closely the prestige ship. This can be explained by the fact that a high pumping power would clean the pollutant before it comes close to the coast.

For the case of the second formulation that forces the optimal trajectory to remain near the coast, independently of the pumping power, the optimal trajectories are much more efficient in cleaning the polluted coast areas than the trajectory that simply follows the Prestige ship.

Furthermore, if the option of using two skimmer ships with high pumping power is available, a good option is to use one skimmer

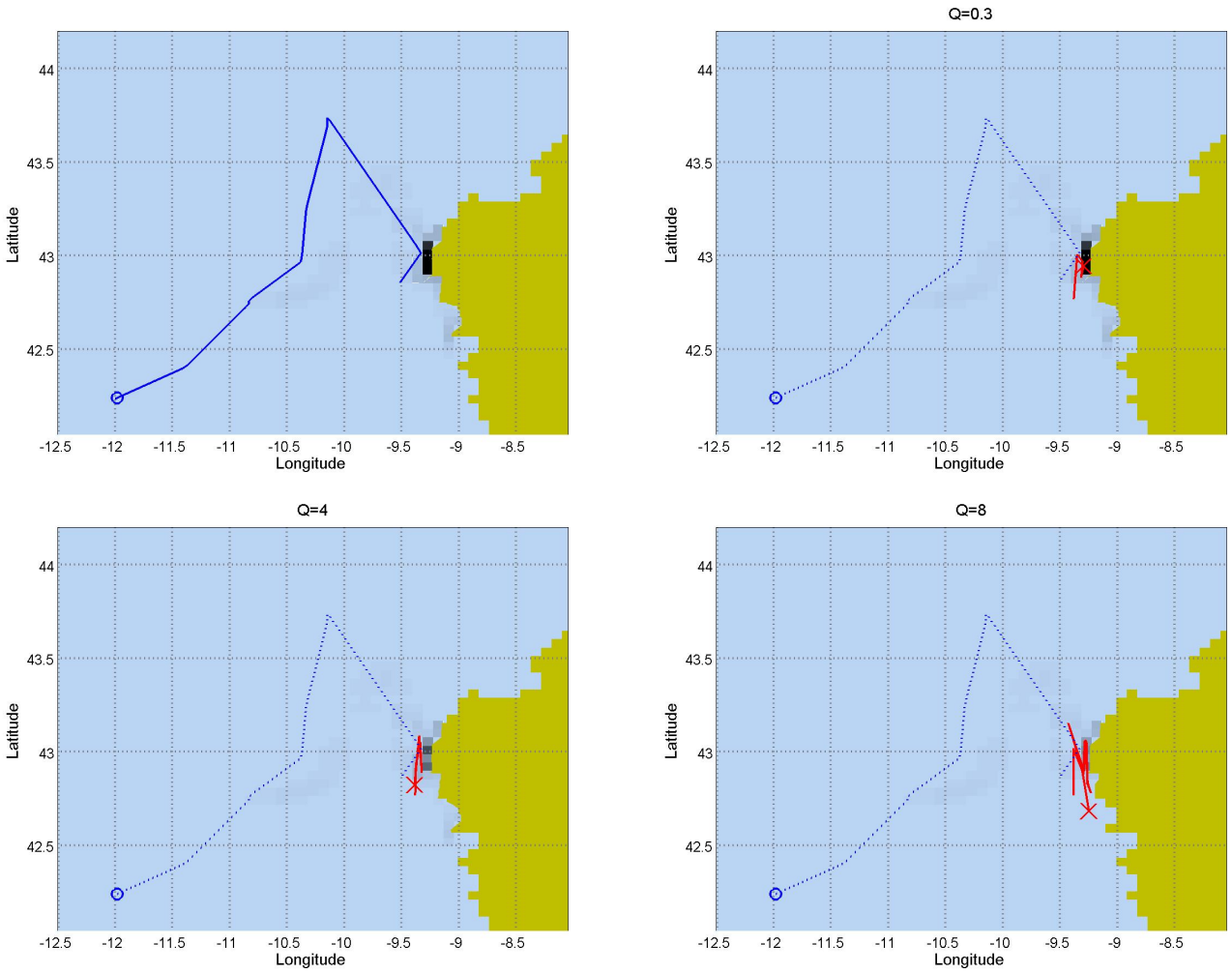

Figure 6: Top view of the final weighted oil concentration distribution c_w, defined in 5.2.2, at 19 November 2002, skimmer ship trajectory (continuous red line), final position of the skimmer ship (x) and final position of the Prestige ship (o) for the experiments: (Top-Left) trajectory of the Prestige ship (continuous blue line) with no pumping process, (Top-Right) OPT-0.3-(4), (Bottom-Left) OPT-4-(4) and (Bottom Right) OPT-8-(4). The trajectory of the Prestige ship is also presented in dotted blue line.

ship near the coast following the optimal trajectory and another one following the polluting ship. In this case our results show that we can clean 88 percent of the pollutant oil.

Future work will focus on the optimization of the trajectory of various skimmer ships at the same time.

Acknowledgment

This work was carried out thanks to the financial support of the Spanish "Ministry of Economy and Competitiveness" under project MTM2011-22658; the research group MOMAT (Ref. 910480) supported by "Banco Santander" and "Universidad Complutense de Madrid"; the "Junta de Andalucía" and the European Regional Development Fund through project P12-TIC301; and the PAPIIT project of the National University of Mexico.

References

1. A.J. Abascal, S. Castanedo, F.J. Mendez, R. Medina, and I.J. Losada, Calibration of a Lagrangian Transport Model Using Drifting Buoys Deployed during the Prestige Oil Spill, Journal of Coastal Research, 251 (2009), 80–90.

2. C. Alavani, R. Glowinski, S. Gomez, B. Ivorra, P. Joshi, A.M. Ramos, Modelling and simulation of a polluted water pumping process, Mathematical and Computer Modelling, 51 (2010), 461–472.

3. AukeVisser. Historical Tankers Site. A-Whale characteristics.
Available at: `http://www.aukevisser.nl/supertankers/bulkers/id453.htm`

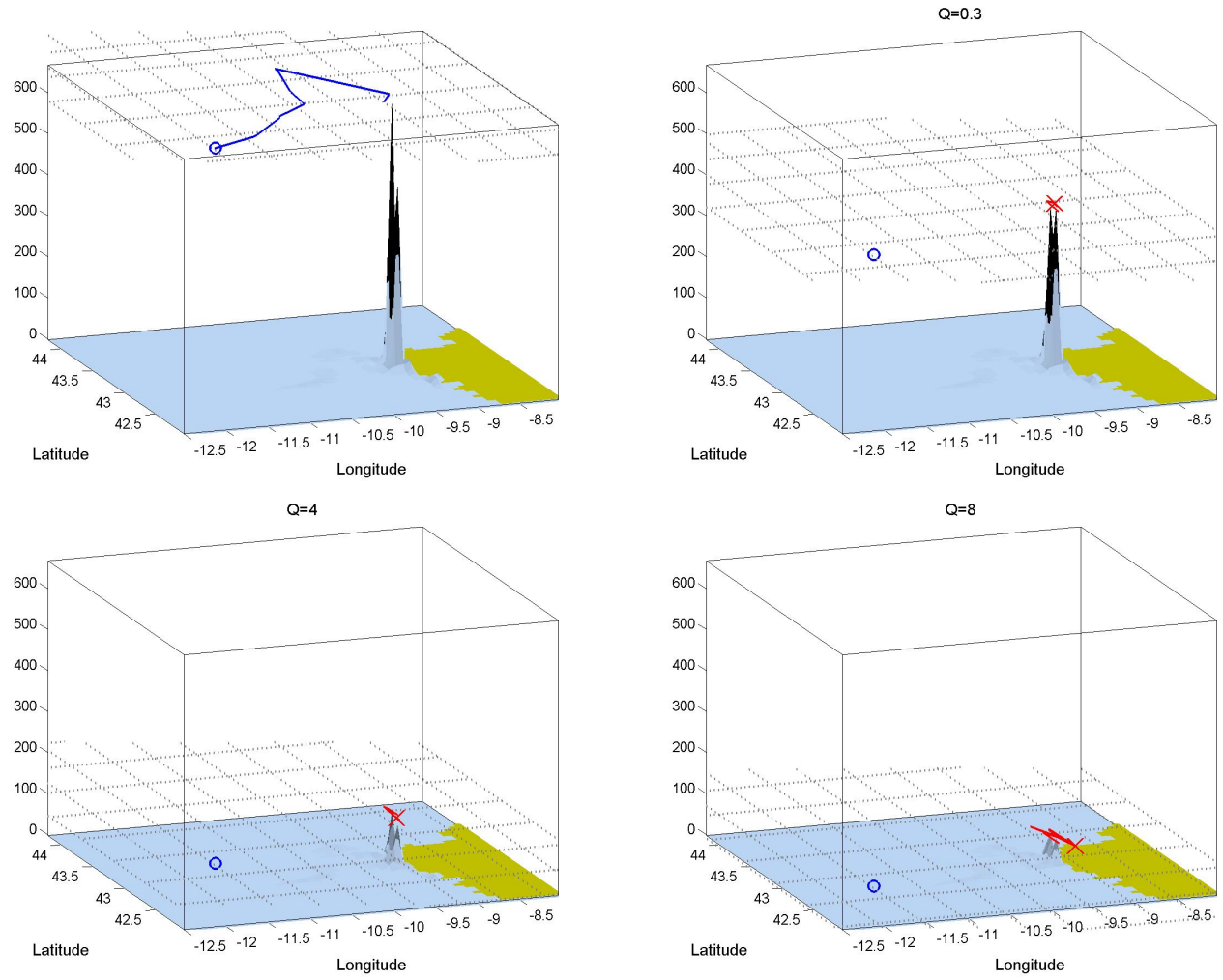

Figure 7: 3D view of the final weighted oil concentration distribution c_w, defined in 5.2.2, at the 19th of November 2002 for the experiments: (Top-Left) no pumping process, (Top-Right) OPT-0.3-(4), (Bottom-Left) OPT-4-(4) and (Bottom Right) OPT-8-(4). A plane at the same height as the maximum value of the oil concentration is also presented. In this plane the skimmer ship trajectory (continuous red line), the Prestige ship trajectory with no pumping process (continuous blue line), final position of the skimmer ship (x) and final position of the Prestige ship (o) are depicted.

4. C.F. Balseiro, P. Carracedo, B. Gmez, P.C. Leito, P. Montero, L. Naranjo, E. Penabad, V. Prez-Muuzuri, Tracking the Prestige oil spill: An operational experience in simulation at MeteoGalicia, Weather, 58(12): 452-458, 2003.

5. A.D. Carpenter, R.G. Dragnich, Marine Operations and Logistics During the Exxon Valdez Spill Cleanup, Oil Spill Conference Proceedings 1991, pp. 205-211, 1991.

6. S. Castanedo, R. Medina, I.J. Losada, C. Vidal, F.J. Mndez, J. Osorio, A. Puente, The Prestige oil spill in Cantabria (Bay of Biscay). Part I: Operational forecasting system for quick response, risk assessment and protection of natural resources, Journal Of Coastal Research, 22(6) (2006), 1474–1489.

7. P.S. Daling, M.O. Moldestad, The Prestige Oil-Weathering Properties. Marine Environmental Technology. 2 (2003), 1–4.

8. T. Drago, Prestige Oil Spill Was Costliest Sea Disaster In History, Albion Monitor, 2003. Available at: `http://www.albionmonitor.com/0307a/copyright/prestigespillcost.html`

9. R. Glowinski, P. Neittaanmaki, Partial Differential Equations. Modelling and Numerical Simulation, Series: Computational Methods in Applied Sciences, Springer,16, 2008.

10. S. Gomez, G. Fuentes, R. Camacho, M. Vasquez, J. M. Otero, A. Mesejo, N. del Castillo, Application of an Evolutionary Algorithm in well test characterization of Naturally Fractured Vuggy Reservoirs, Society of Petroleum Engineering, SPE No. 103931, 2006.

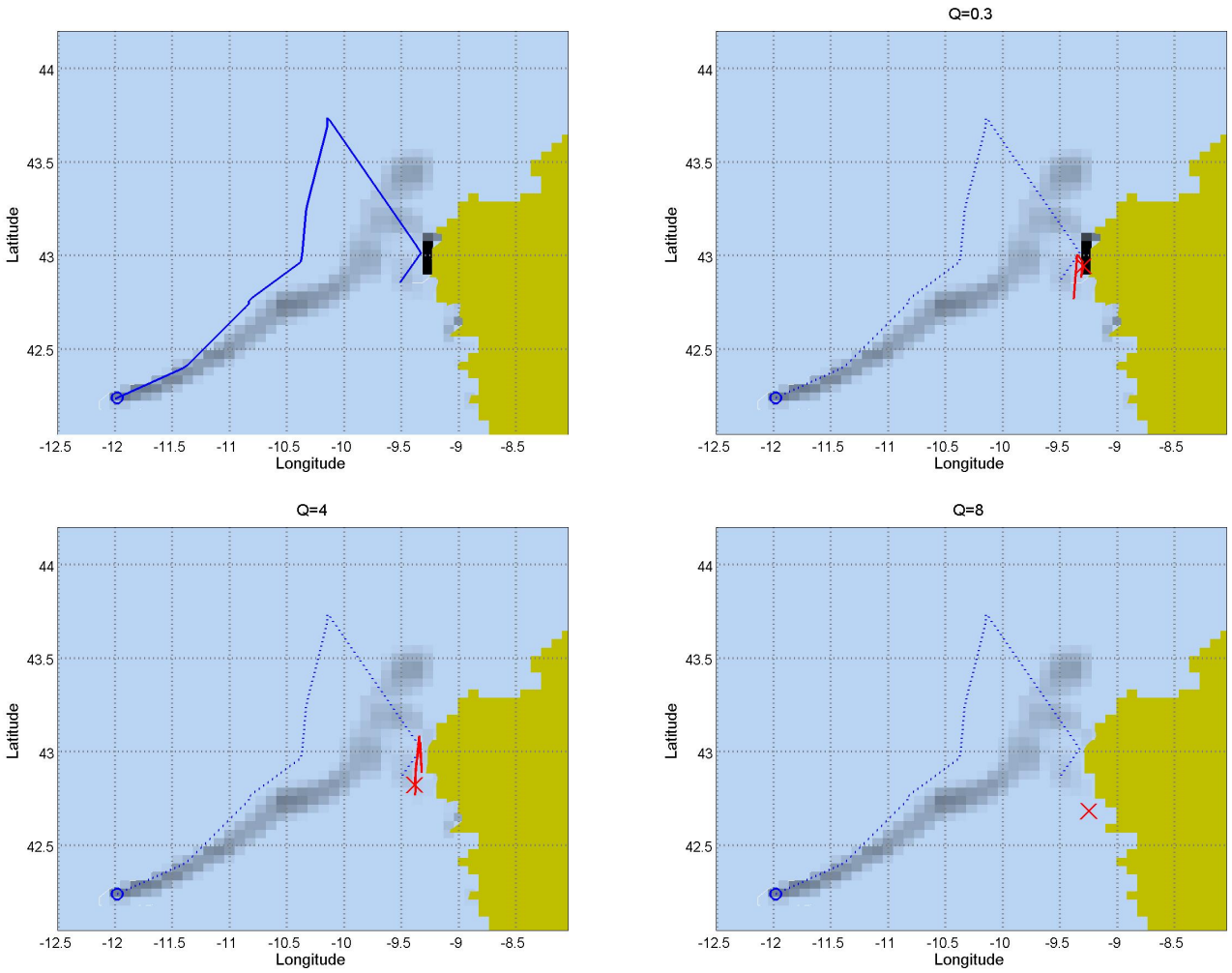

Figure 8: Top view of the final oil concentration distribution at 19 November 2002, skimmer ship trajectory (continuous red line), final position of the skimmer ship (x) and final position of the Prestige ship (o) for the experiments: (Top-Left) trajectory of the Prestige ship (continuous blue line) with no pumping process, (Top-Right) OPT-0.3-(4), (Bottom-Left) OPT-4-(4) and (Bottom Right) OPT-8-(4). The trajectory of the Prestige ship is also presented in dotted blue line.

11. S. Gomez, B. Ivorra, A.M. Ramos, Optimization of a pumping ship trajectory to clean oil contamination in the open sea, Mathematical and Computer Modelling, 54(1) (2011), 477-489.

12. S. Gomez, G. Severino, L. Randazzo, G. Toraldo, J.M. Otero., Identification of the hydraulic conductivity using a global optimization method, Agricultural Water Management, 93(3) (2009), 504–510.

13. B. Ivorra, S. Gomez,R. Glowinski , A.M. Ramos,Nonlinear Diffussion-Advection-Reaction Phenomena Involved in the Pumping of Oil from Open Sea: Modeling and Numerical Simulation, Eprints de la Universidad Complutense de Madrid, 29301, Submitted to a peer review journal, 2015. Available at: `http://eprints.ucm.es/29301`

14. Ivorra, B., Hertzog, D. E., Mohammadi, B., and Santiago, J. G. (2006). Semi-deterministic and genetic algorithms for global optimization of microfluidic protein-folding devices. *International Journal for Numerical Methods in Engineering*, 66(2):319–333.

15. Ivorra, B., Mohammadi, B., and Ramos, A. (2009). Optimization strategies in credit portfolio management. *Journal of Global Optimization*, 43(2-3):415–427.

16. Ivorra, B., Mohammadi, B., and Ramos, A. (2014). Design of code division multiple access filters based on sampled fiber bragg grating by using global optimization algorithms. *Optimization and Engineering*, 15(3):677–695.

17. Ivorra, B., Ramos, A., and Mohammadi, B. (2007). Semideterministic global optimization method: Application to a control problem of the burgers equation. *Journal of Optimization Theory and Applications*, 135(3):549–561.

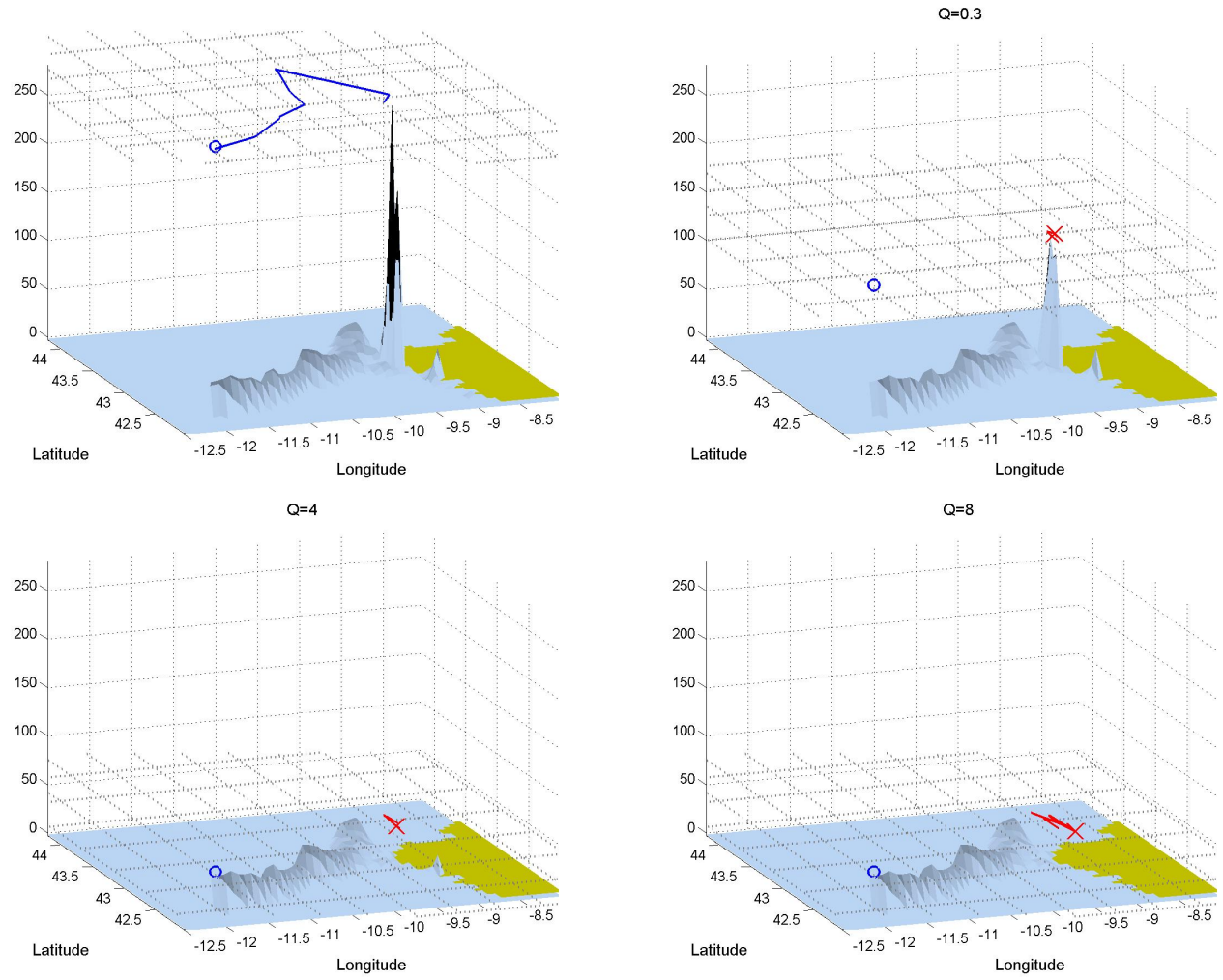

Figure 9: 3D view of the final oil concentration distribution on the 19th of November 2002 for the experiments: (Top-Left) no pumping process, (Top-Right) OPT-0.3-(4), (Bottom-Left) OPT-4-(4) and (Bottom Right) OPT-8-(4). A plane at the same height as the maximum value of the oil concentration is also presented. In this plane the skimmer ship trajectory (continuous red line), the Prestige ship trajectory with no pumping process(continuous blue line), final position of the skimmer ship (x) and final position of the Prestige ship (o) are depicted.

18. M. L. Loureiro, A. Ribas, E. Lpez, E. Ojea, Estimated costs and admissible claims linked to the Prestige oil spill, Ecological Economics, 59(1) : 48-623, 2006.

19. Merv Fingas. The Basics of Oil Spill Cleanup, Second Edition, CRC Press, 2000.

20. P. Montero, J. Blanco, J.M. Cabanas, J. Maneiro, Y. Pazos, A. Moroo, C.F. Balseiro, P. Carracedo, B. Gmez, E. Penabad, V. Perez-Muuzuri, F. Braunschweig, R. Fernades, P.C. Leitao and R. Neves. Oil Spill Monitoring, Forecasting on the Prestige-Nassau accident. In: Proceedings 26th Arctic Marine Oil Spill Program (AMOP) Technical Seminar, 2 (2003), 1013–1029.

21. N.O.A.A., Oil Spill case histories 1967-1991. Summaries of significant U.S. and international spills, Office of response and restoration of the U.S. National Ocean, Report HMRAD 92-11, 1992.

22. Office of response and restoration of the U.S. National Ocean Service. Website: `http://response.restoration.noaa.gov`

23. Office of response and restoration of the U.S. National Ocean Service, Incident News Home. Website: `http://incidentnews.gov`

24. Rocha, M. and Neves, J. (1999). Preventing premature convergence to local optima in genetic algorithms via random offspring generation. In Imam, I., Kodratoff, Y., El-Dessouki, A., and Ali, M., editors, *Multiple Approaches to Intelligent Systems*, volume 1611 of *Lecture Notes in Computer Science*, pages 127–136. Springer Berlin Heidelberg.

25. S.K. Skinner, W.K. Reilly, The Exxon Valdez Oil Spill. National Response Team, 2008.

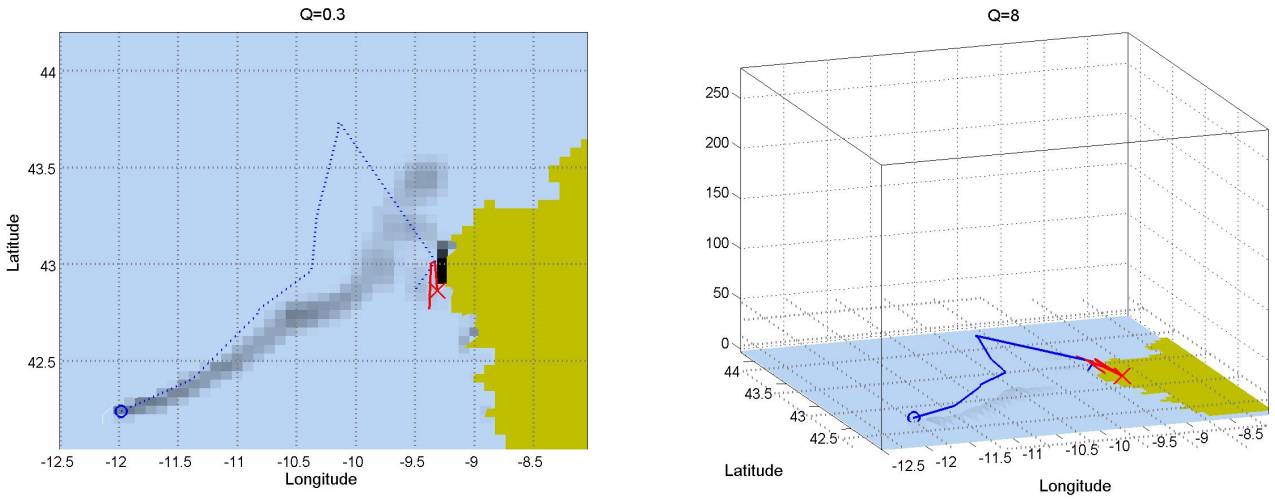

Figure 10: (Left) Top view and (Right) 3D view of the final oil concentration distribution at 19th of November 2002, skimmer ship trajectory (continuous line), final position of the skimmer ship (x) and final position of the Prestige ship (o) for the experiments with two skimmer ships, one following the trajectory generated by OPT-8-(4) and another one following the Prestige ship trajectory. The trajectory of the prestige ship is also presented in dotted line. In the 3D view case, a plane at the same height as the maximum value of the oil concentration is also presented. In this plane the skimmer ship trajectory (continuous line), Prestige ship trajectory (dotted line), final position of the skimmer ship (x) and final position of the Prestige ship (o) are depicted.

26. D. Di Serafino, S. Gomez, L. Milano, F. Riccio and G. Toraldo, A genetic algorithm for a global optimization problem arising in the detection of gravitational waves, Journal of Global Optimization, 48(1) (2010), 41–55.

27. United States Environmental Protection Agency, Oil Spill Response Techniques, 2009. Website: http://www.epa.gov/osweroe1/content/learning/oiltech.htm